Fermi National Accelerator Laboratory

FERMILAB-TM-1997

An Imaginary-γ_t Lattice With Dispersion-Free Straights for the 50 GeV High-Intensity Proton Synchrotron

King-Yuen Ng

Fermi National Accelerator Laboratory
P.O. Box 500, Batavia, Illinois 60510

February 1997

Operated by Universities Research Association Inc. under Contract No. DE-AC02-76CH03000 with the United States Department of Energy

Disclaimer

Distribution

TM 1997

AN IMAGINARY-γ_t LATTICE WITH DISPERSION-FREE STRAIGHTS FOR THE 50 GeV HIGH-INTENSITY PROTON SYNCHROTRON

King-Yuen Ng

Fermi National Accelerator Laboratory, Batavia, IL 60510

(February, 1997)

Abstract

During polarized beam experiments, the 50 GeV proton synchrotron, proposed by the Institute of Nuclear Study of Japan, requires zero-dispersion straight sections. This will be implemented by turning on a special excitation of the quadrupoles resulting in a dispersion wave through the arcs of the machine. Aside from the inconvenience of the power supply, this special excitation also brings about unwanted high betatron functions and high dispersion functions, which will eventually limit the performance of the accelerator at high intensities. In this paper, dispersion suppressors are introduced. A new preliminary lattice that contains two straight sections with nonzero dispersion and two straight sections with zero dispersion is presented. The whole ring remains having a reasonable imaginary γ_t. The horizontal and vertical betatron functions have been kept to below 32.4 m and dispersion function between -0.52 and 1.86 m. The number of 6.2 m dipoles is reduced from 96 to 92, and the dipole field at 50 GeV will become slightly above 18 T. Some analysis of the new lattice is discussed.

I INTRODUCTION

In order to reduce beam loss, the 50-GeV proton synchrotron of the Japan Hadron Project (JHP) designed by the Institute for Nuclear Study of Japan (INS) will operate with an imaginary-γ_t [1]. The flexible momentum-compaction (FMC) modules [2] in the lattice are roughly 3 FODO-cell long. The lattice is 4-fold symmetric. Each quadrant consists of 6 FMC modules and a long straight section of about 60 m in length. The dispersion in the long straight section varies between -0.71 and 0.58 m. Although the dispersion is small, it is always more appealing to have zero-dispersion straights. This is especially true when the synchrotron is accelerating polarized beam. To obtain zero dispersion in one straight section and another on the other side of the ring, a special excitation of the quadrupoles needs to be turned on so as to allow a dispersion wave and a betatron wave to flow through half of the ring. Aside from the inconvenience of having a special power supply, this excitation also brings about unwanted high betatron functions and high dispersion functions, which will eventually limit the performance of the accelerator at high intensities. In this paper, we suggest the introduction of dispersion suppressors. A new preliminary lattice that contains two straight sections with nonzero dispersion and two straight sections with zero dispersion is presented.

II DISPERSION SUPPRESSOR

The standard FMC module of the JHP ring is shown in Fig. 1 with its lattice elements, betatron functions and dispersion. To study its dispersion property, we go to the normalized dispersion space (ξ-χ), where

$$\xi = \sqrt{\beta_x} D' - \frac{\beta_x' D}{2\sqrt{\beta_x}} = \sqrt{2J}\cos\phi \ , \quad \chi = \frac{D}{\sqrt{\beta_x}} = \sqrt{2J}\sin\phi \ . \tag{2.1}$$

Here, D and D' are, respectively, the dispersion function and its derivative with respect to the longitudinal coordinate s, β_x and β_x' are, respectively, the horizontal betatron amplitude function and its derivative, J is the dispersion action, $\sqrt{2J}$ is the amplitude of the normalized dispersion vector, and ϕ is identical to the horizontal Floquet betatron phase advance in the region where there is no dipole. The dispersion function satisfies the second-order inhomogeneous differential equation,

$$D'' + K_x(s)D = \frac{1}{\rho(s)} \ , \tag{2.2}$$

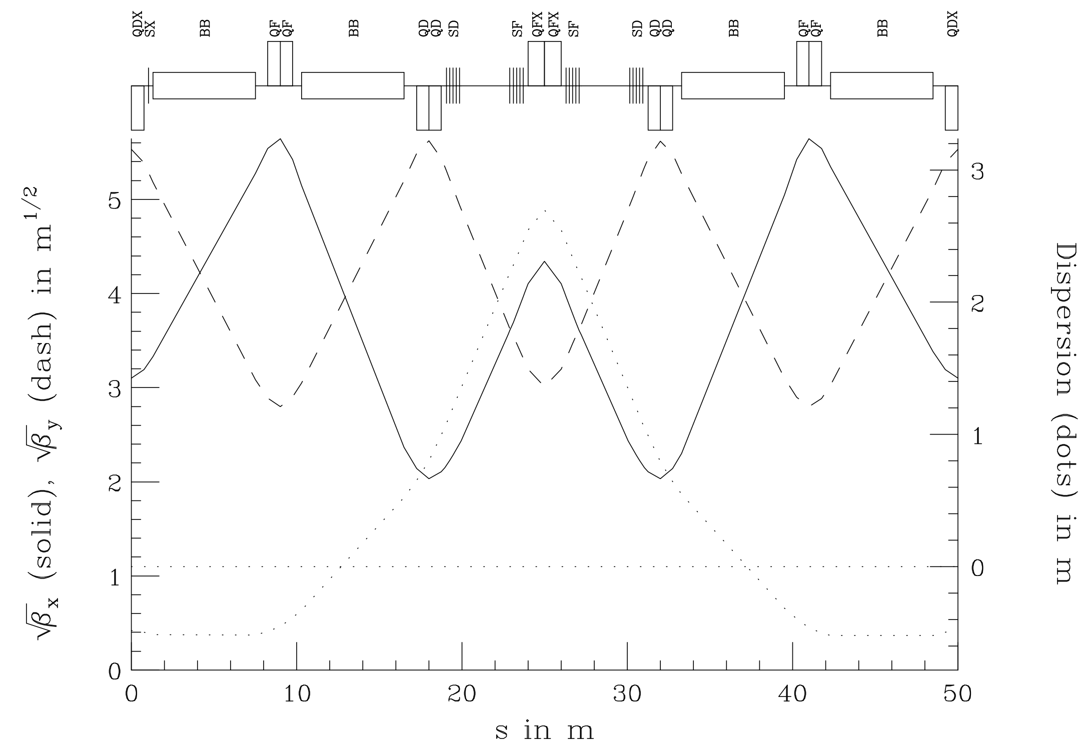

Horizontal tune = 0.74048 + 0.375E+01EX − 0.420E+01EY KSF: 0.04556638
Vertical tune = 0.53074 − 0.420E+01EX + 0.365E+01EY KSD: −0.07517985
Dispersion max/min: 2.69576/−0.52128m, γ_t: (0.00, 27.56)
β_x max/min: 31.84/ 4.12278m, ν_x: 0.74048, ξ_x: 0.28, Module length: 50.0000m
β_y max/min: 31.60/ 7.82463m, ν_y: 0.53074, ξ_y: 0.07, Total bend angle: 0.27318197 rad

Figure 1: The lattice structure of the standard FMC module of the JHP ring.

where $\rho(s)$ is the local radius of curvature, and

$$K_x = \frac{1}{\rho^2} - \frac{1}{B\rho}\frac{\partial B_y}{\partial x} \ , \tag{2.3}$$

is the sum of the quadrupole and centrifugal focusing. In the thin-element approximation, Eq. (2.2) indicates that $\Delta D = 0$ and $\Delta D' = \theta$ in passing through a thin dipole with bending angle θ. Therefore, in the normalized ξ-χ space, the normalized dispersion vector changes by $\Delta\xi = \sqrt{\beta_x}\theta$ and $\Delta\chi = 0$. Outside the dipoles ($\rho = \infty$), the dispersion function satisfies the homogeneous equation, so that J is an invariant, with ξ and χ satisfying $\xi^2 + \chi^2 = 2J$, which is a circle, and the normalized dispersion vector advances by an angle ϕ equal to the betatron phase advance. The dispersion

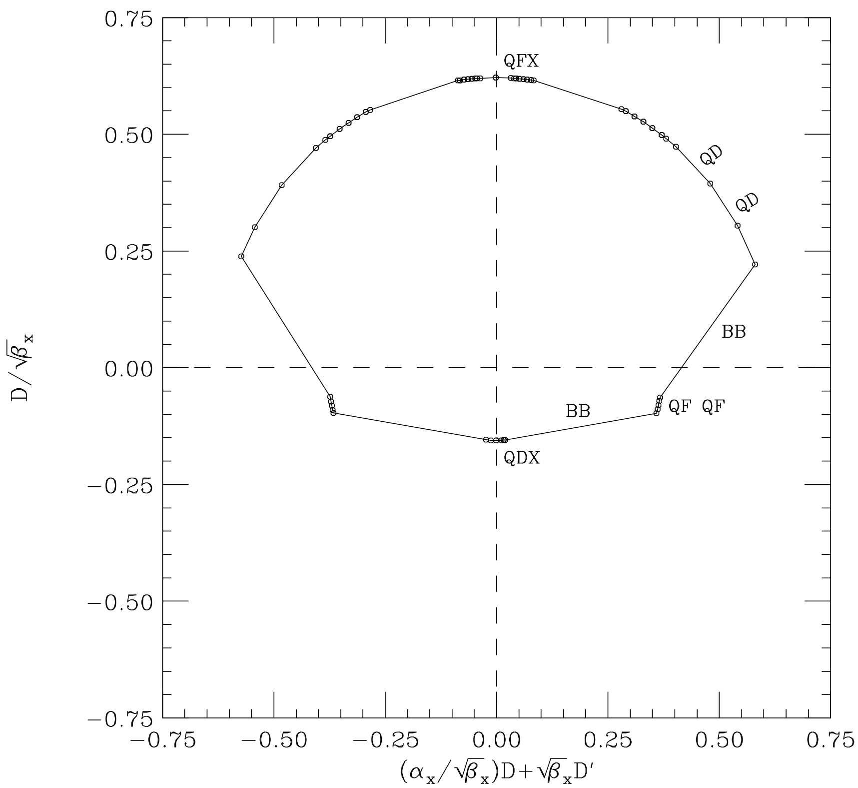

Figure 2: The standard FMC module of the JHP ring plotted in the normalized dispersion plane.

plot of the FMC module in Fig. 1 is given in Fig. 2. We see that the module starts off from the quadrupole QDX with zero β_x' and D'. The dispersion is -0.5213 m. The first dipole BB is represented by a long straight line pointing mostly to the right. Note that this line is not exactly horizontal, because the dipole is far from a thin element and there is a phase advance associated. If we chop up the dipoles into smaller elements, this straight line will be curved. However, it will still be quite different from the arc of a circle with center at the origin of the plot. The deviation just represents the angle-bending nature of the dipole. Next come the quadrupoles QF and the second dipole BB. After that there is no more dipole and the plot until the center quadrupole QFX just follows the arc of a circle centered at the origin. The other half of the module is just the mirror image of the first half.

In order to be a dispersion suppressor, we must alter the lattice so that the end of the module stops precisely at the origin of the dispersion space. To accomplish this, we must first make the radius of the arc smaller in the upper half of the dispersion plane, and second we must use an exact amount of dipole to bring the module to $D = 0$ and $D' = 0$ at the point when the arc reaches roughly 180°. The suppressor constructed in this way is shown in Fig. 3 and its dispersion plot in Fig. 4. The construction

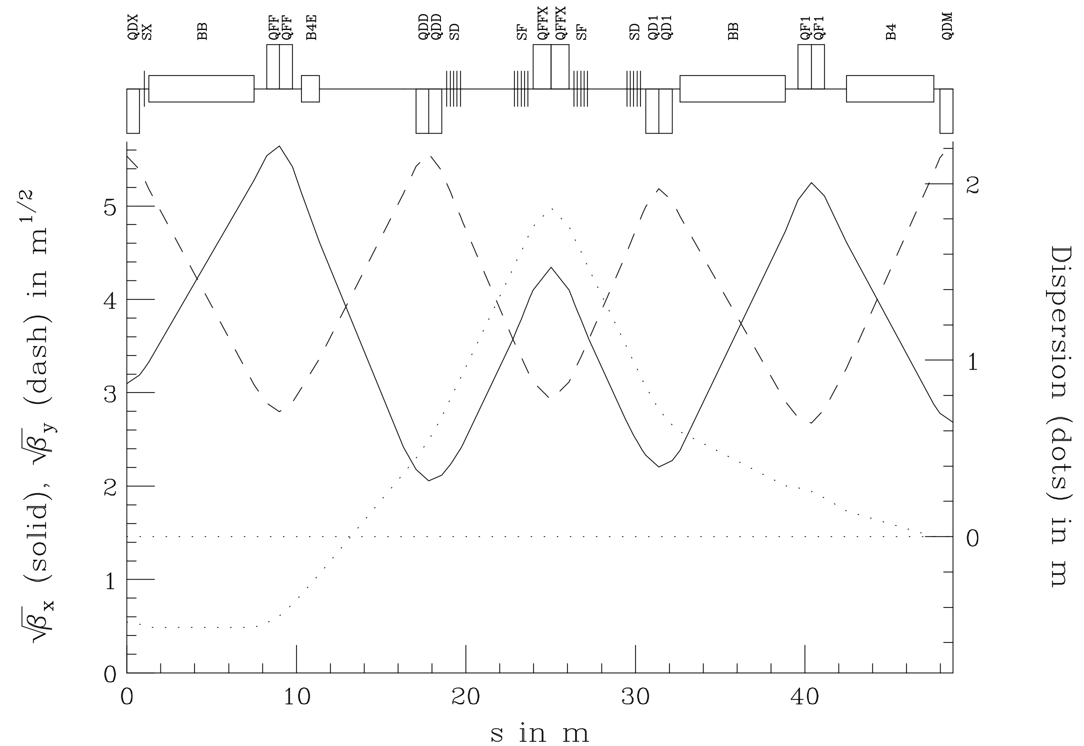

Horizontal tune = 0.72094 + 0.458E+01EX − 0.188E+01EY   KSF: 0.06804036
Vertical tune = 0.54478 − 0.188E+01EX + 0.307E+01EY   KSD: −0.10894394
Dispersion max/min: 1.86319/−0.51480m, γ_t: (0.00, 69.05)
β_x max/min: 31.84/ 4.22486m, ν_x: 0.72094, ξ_x: 0.47,   Module length: 48.7269m
β_y max/min: 32.32/ 7.16567m, ν_y: 0.54478, ξ_y: 0.43,   Total bend angle: 0.20488648 rad

Figure 3: The lattice structure of the dispersion suppressor.

starts from the pulling out the second dipole, so that the module continues with a much smaller arc until the quadrupole QFFX. To facilitate lattice computation, we treat this as a point of symmetry, that is with $\beta'_x = \beta'_y = D' = 0$, although these constraints are not necessary. After that we continue as in the case of the standard FMC module with the exception that the last dipole, called B4, is shortened so that the module lands exactly at $D = D' = 0$. In order not to deal with a fractional

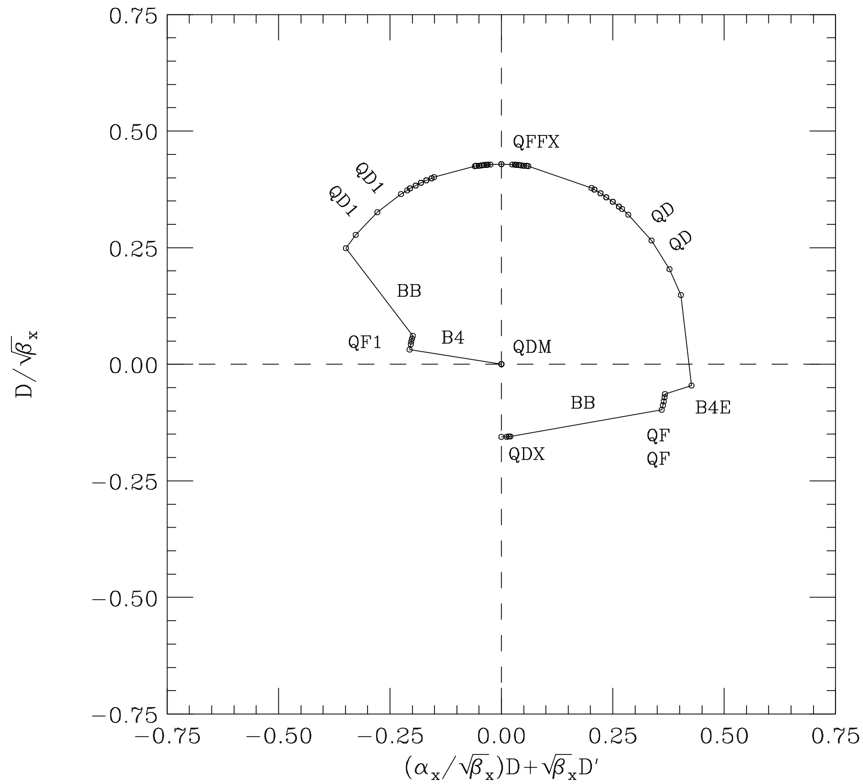

Figure 4: The dispersion suppressor plotted in the normalized dispersion plane.

dipole, the amount B4 has been shortened, called B4E, is placed in the space where the second dipole has been pulled out. In other words, one normal dipole has been pulled out, and another normal dipole has been chopped up into two parts B4 and B4E. The chopping up of a normal dipole for the dispersion suppressor seems to be inevitable. This is very similar to the situation of the dispersion suppressor in a FODO-cell lattice, where one can avoid chopping up dipole only when the phase advance of each cell is exactly $\pi/3$. In this present dispersion suppressor, B4 and B4E have been made 83% and 17% of the normal bending dipole BB.

As shown in Fig. 3, the dispersion suppressor is not very much different from the standard FMC module, aside from the fact that one dipole is missing and that the dispersion winds down to zero. The suppressor has a length of 48.7269 m, maximum/minimum dispersion of $1.8632/-0.5148$ m, maximum/minimum horizontal betatron function 31.84/4.22 m and maximum/minimum vertical betatron function

32.32/7.17 m. The vertical and horizontal tune advances are 0.721/0.545, which are very close to the 0.740/0.531 for the standard FMC module. Best of all, this suppressor has also an imaginary transition gamma of $\gamma_t = 69.05i$, so that the whole ring can still retain its imaginary-γ_t property.

The whole ring has now only 92 dipoles each of length 6.2 m. Since the beam particles are to be accelerated to the maximum total energy of 50 GeV, the maximum bending field of the dipole becomes 1.837 T, which is high but is still possible.

III LONG STRAIGHT SECTIONS

There will be two long straight sections that are dispersion-free and two that are not. The long straight section that has nonzero dispersion joins two standard FMC modules together. This is the same type of long straight sections in the original design of the JHP synchrotron. In this design, this straight is illustrated in Fig. 5, with a length chosen to be 61.2524 m. In the dispersion plane of Fig. 2, this long straight section is just represented by a circle centered at the origin, starting from the quadrupole QDX and back to the same quadrupole. This can be understood easily from Eq. (2.2), since no dipoles are present.

The zero-dispersion straight shown in Fig. 6 can be constructed in the same way. It has a length of 62.2938 m. Since both the dispersion and its derivative are zero, this straight is represented as only one dot, namely the origin in the dispersion plane of Fig. 4.

Now the whole ring can be assembled. We start from the center of the non-dispersion-free straight section, then 5 standard FMC modules, the dispersion suppressor, and then the dispersion-free long straight section. We make a mirror reflection about the center of the dispersion-free straight to arrive back to the center of the other non-dispersion-free straight. This complete one half of the ring. The SYNCH input file for the lattice is listed in the Appendix.

IV SEXTUPOLE CORRECTION

In general, quadrupoles of the FMC modules are of larger integrated strength than those in the usual FODO lattice. As a result, larger natural chromaticities will be

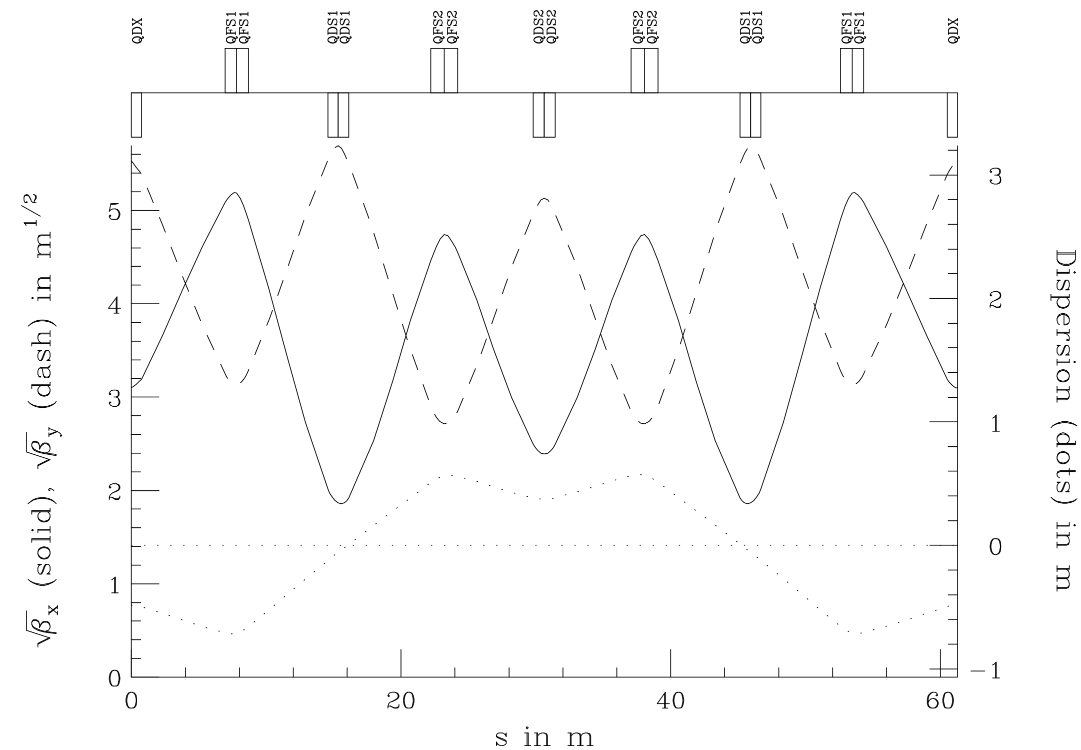

Dispersion max/min: 0.56669/−0.71118m,
β_x max/min: 26.90/ 3.48443m, ν_x: 1.00000, ξ_x: −1.18, Module length: 61.2524m
β_y max/min: 32.40/ 7.36765m, ν_y: 0.64504, ξ_y: −0.93, Total bend angle: 0.000000 rad

Figure 5: The lattice structure of the long straight section with dispersion.

generated and sextupoles of larger strengths will be required for their corrections. The corrections are mainly made by the two families of sextupoles SF and SD as shown in Figs. 1 and 3. There each SF or SD is represented by 5 thin sextupoles in the lattice code. Just after the entrance defocusing quadrupole of each FMC module, there is a third family SX, which is used for fine adjustment. For example, the chromaticity corrections have been made by setting the strength of each SX to be 0.105 m^{-2} and each of the thin SF and SD 0.0572 m^{-2} and -0.0933 m^{-2}, respectively. The resulting amplitude dependence on tunes are

$$\nu_x = 21.0954 + 130\frac{\epsilon_x}{\pi} - 116\frac{\epsilon_y}{\pi} \ ,$$

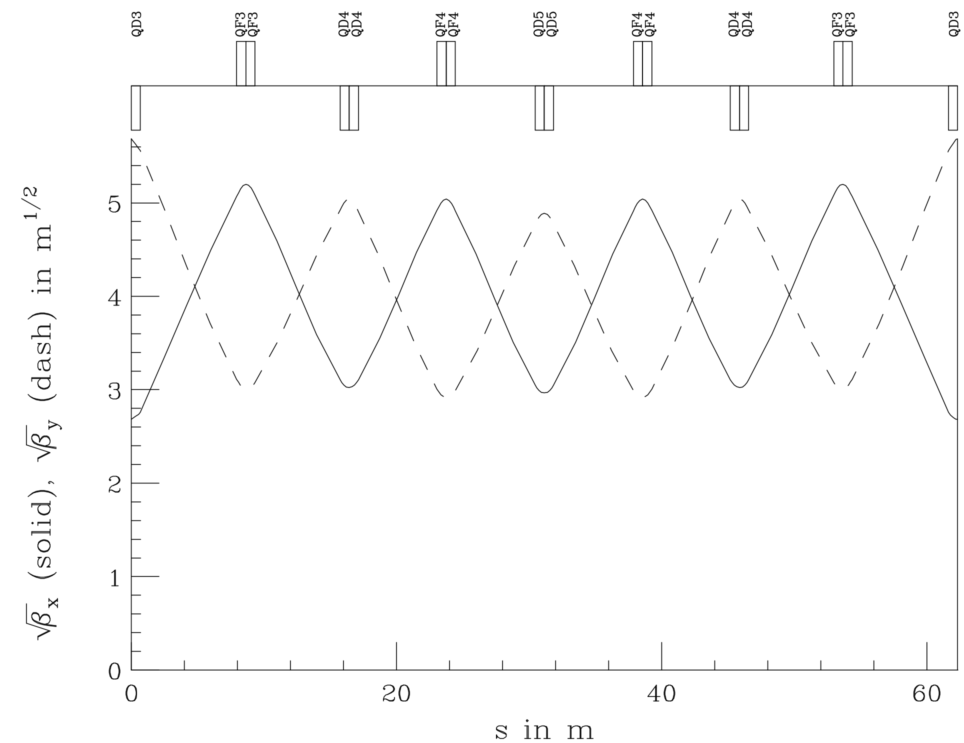

Dispersion max/min: 0.00000/ 0.00000m, γ_t: (0.00, 0.00)
β_x max/min: 27.04/ 7.21283m, ν_x: 0.70100, Module length: 62.2938m
β_y max/min: 32.32/ 8.50019m, ν_y: 0.67969, Total bend angle: 0.00000000 rad

Figure 6: The lattice structure of the long straight section that is dispersion-free.

$$\nu_y = 15.4433 - 116\frac{\epsilon_x}{\pi} + 134\frac{\epsilon_y}{\pi} \ , \tag{4.1}$$

where the emittances ϵ_x and ϵ_y are measured in m. The magnitude of the third family of sextupoles has been varied so as to make the 3 different detunings as close as possible in magnitude and that they have the desirable signs. We see that with $\epsilon_x = \epsilon_y = 50\pi \times 10^{-6}$ m, the largest tune spread is only 0.0067, which is certainly acceptable for a non-storage ring [4].

Another measure of nonlinearity introduced by the correction sextupoles is the single-particle smears, S_x and S_y, which are defined as the fractional rms distortion of the Poincaré torus at any phase advance ψ_x in the horizontal and ψ_y in the vertical phase spaces. In other words,

$$S_x(\psi_x,\psi_y)=\left(\frac{\langle(\delta\mathcal{A}_x)^2\rangle}{\mathcal{A}_x^2}\right)^{1/2}\;, \qquad S_y(\psi_x,\psi_y)=\left(\frac{\langle(\delta\mathcal{A}_y)^2\rangle}{\mathcal{A}_y^2}\right)^{1/2}\;. \tag{4.2}$$

where the amplitudes $\mathcal{A}_x$ and $\mathcal{A}_y$ are related to the emittances through

$$\epsilon_x=\frac{\pi\mathcal{A}_x^2}{\beta_0}\,, \qquad \epsilon_y=\frac{\pi\mathcal{A}_y^2}{\beta_0}\,. \tag{4.3}$$

Here β_0 is just some reference betatron function for dimensional purpose and can be set arbitrarily to 1 m for convenience. The single-particle smears [3] can then be computed easily in terms of the 5 pairs of distortion functions (B_1,A_1), (B_3A_3), $(\bar{B},\bar{A})$, (B_+,A_+), and (B_-,A_-) [5, 6, 7, 8]:

$$\begin{aligned} S_x^2 &= \tfrac{1}{2}\mathcal{A}_x^2(A_3^2+B_3^2+A_1^2+B_1^2)-2\mathcal{A}_y^2(A_1\bar{A}+B_1\bar{B}) \\ &\quad +\frac{\mathcal{A}_y^4}{2\mathcal{A}_x^2}(A_+^2+B_+^2+A_-^2+B_-^2+4\bar{A}^2+4\bar{B}^2)\;, \\ S_y^2 &= 2\mathcal{A}_y^2(A_+^2+B_+^2+A_-^2+B_-^2)\;. \end{aligned} \tag{4.4}$$

The distortion functions are, of course, functions of the sextupoles, whose integrated strengths are

$$s_k=\lim_{\ell\to 0}\left[\left(\frac{\beta_x^3}{\beta_0}\right)^{1/2}\frac{B_y''\ell}{2(B\rho)}\right]_k\;, \qquad \bar{s}_k=\lim_{\ell\to 0}\left[\left(\frac{\beta_x\beta_y^2}{\beta_0}\right)^{1/2}\frac{B_y''\ell}{2(B\rho)}\right]_k\;, \tag{4.5}$$

which depend also on the reference betatron function β_0. The horizontal and vertical smears are plotted in Fig. 7. We see that the rms vertical smear reaches only about 0.1%, which is very small, and the horizontal smear is still smaller. The full smears will be roughly $\sqrt{2}$ times the rms values, which are much less than the 7% nonlinear criterion of the former Superconducting Super Collider [4]. We also see that the smears are step-like, constant over a region and exhibiting a jump only when a sextupole is encountered.

V BETATRON BEATINGS

In this FMC-type lattice, it is impossible to place a sextupole beside every quadrupole to correct for local chromaticities. As a result, particles with a momentum

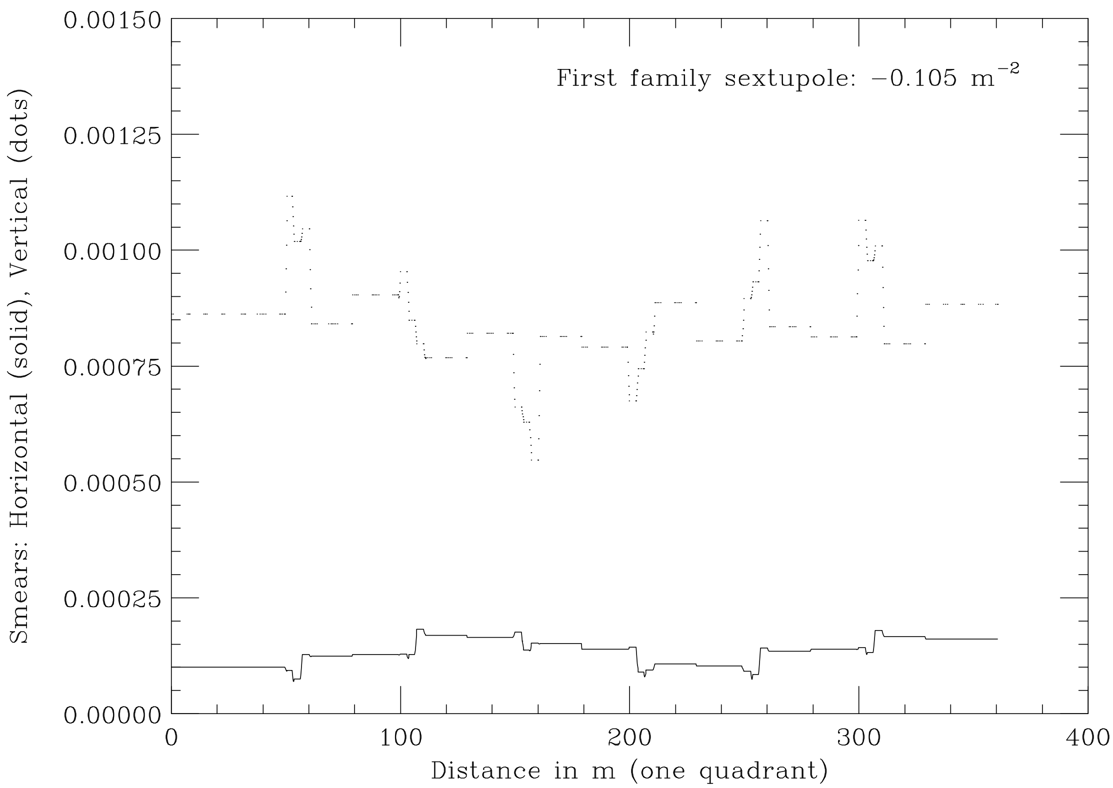

Figure 7: The horizontal and vertical single-particle smears for one quarter of the accelerator ring.

offset δ will see a different set of betatron functions. The fractional changes in the betatron functions per unit momentum deviation are called "beat factors". At phase advance ψ, they are given by [9]

$$\left.\frac{\Delta\beta}{\beta}\right|_{\psi} = -\frac{1}{2\sin 2\pi\nu}\int_{\psi}^{\psi+2\pi\nu} k(\psi')\beta^2(\psi')\cos 2(\pi\nu+\psi-\psi')d\psi' \; . \tag{5.1}$$

In the above, the phase advance ψ, field gradient k, and tune ν assume their horizontal or vertical values for the horizontal or vertical beat factor.

The beat factor can be made complex by introducing the imaginary part

$$-\left.\frac{d}{d\psi}\frac{\Delta\beta}{2\beta}\right|_{\psi} = -\frac{1}{2\sin 2\pi\nu}\int_{\psi}^{\psi+2\pi\nu} k(\psi')\beta^2(\psi')\sin 2(\pi\nu+\psi-\psi')d\psi' \; . \tag{5.2}$$

If we denote the real part by B and the imaginary part by A, the vector (B, A) rotates at a tune of 2ν when there is no field gradient. Whenever it passes through a field gradient k of infinitesimal length ℓ, A increases by

$$\Delta A = -\frac{\beta k \ell}{2} \tag{5.3}$$

while B remains unchanged. Thus the magnitude of the beat vector is an invariant unless it passes through a field gradient. The contribution to the beat factors, however, does not come merely from the field gradient of the quadrupoles alone; there are also contributions from the sextupoles, the centripetal force of the dipoles as well as the edges of the dipoles. The beat factors are plotted in Fig. 8, and the magnitudes of the beat vectors in Fig. 9. The largest beat factor per unit momentum offset

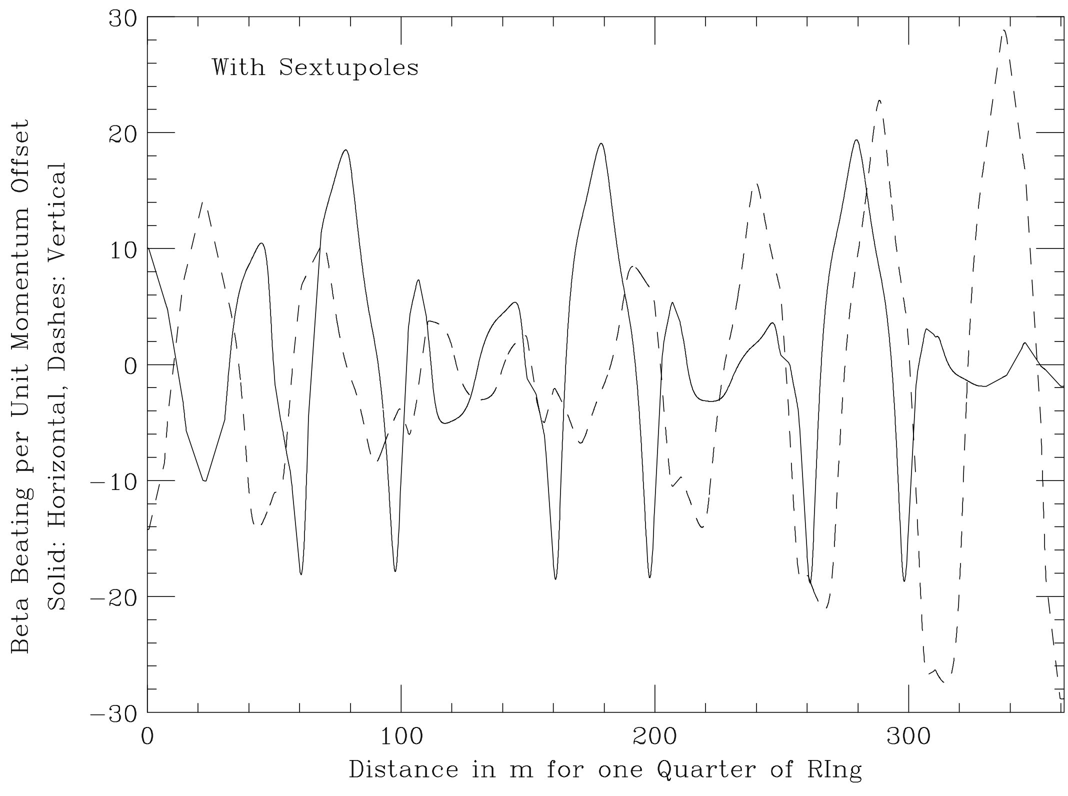

Figure 8: The horizontal and vertical beat factors for one quarter of the accelerator ring.

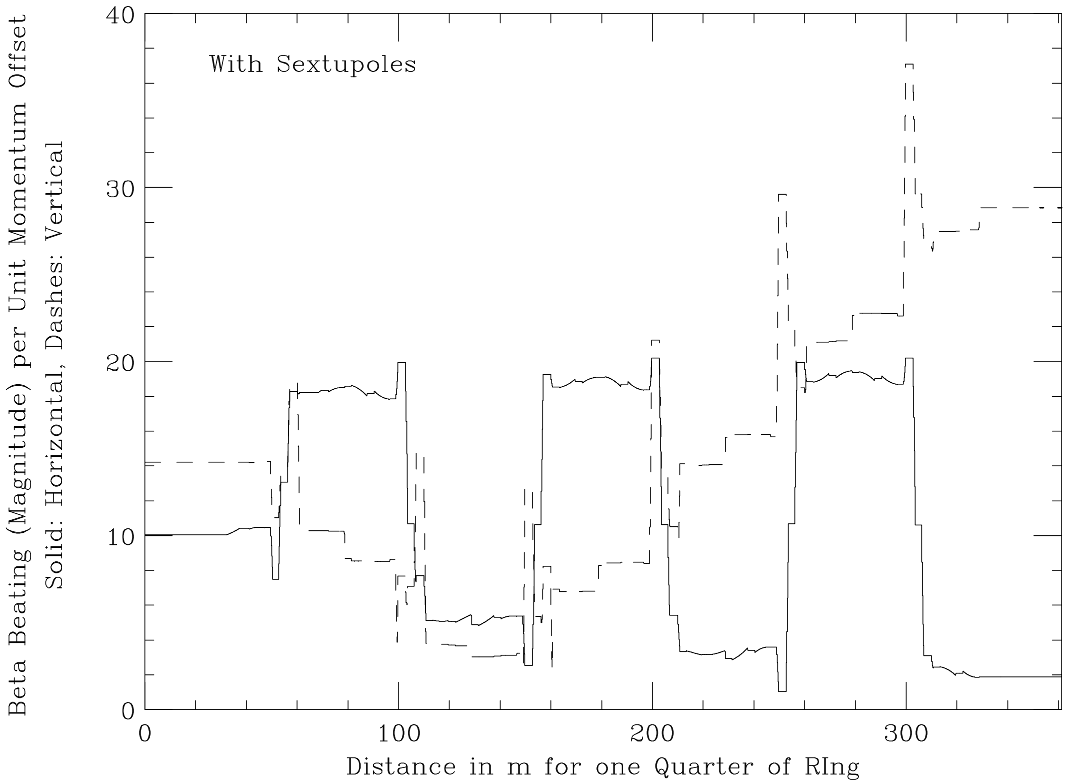

Figure 9: The magnitudes of the horizontal and vertical beating vectors for one quarter of the accelerator ring.

is around 25. Considering that the momentum spread of the beam is only 0.5% at injection, the relative change in betatron function is at the most 10% which is not excessive at all.

The harmonic analysis of the beat factors is also important, because it gives us a clue to reduce the beat factors. For a left-right symmetric lattice, choosing the point of symmetry as the point having zero phase advances, the Courant-Synder J_p's become real. and can be expanded as

$$J_p = \int_{-\pi\nu}^{\pi\nu} k(\psi')\beta^2(\psi')\cos\frac{p\psi'}{\nu}d\psi' \ . \tag{5.4}$$

Then each beat factor can be written as

$$\left.\frac{\Delta\beta}{\beta}\right|_{\psi} = -\frac{J_0}{\pi\nu} - \frac{2\nu}{\pi}\sum_{p>0}\frac{J_p\cos\frac{p\psi'}{\nu}}{4\nu^2-p^2} \ . \tag{5.5}$$

Each half of the INS lattice has a left-right symmetry except for the third family of sextupoles which is placed only at one side of the entrance D-quadrupole of each module. However, the asymmetry is small and so are the $\mathcal{Im}\, J_p$'s. Therefore, we can assume the J_p's to be real.

Since the lattice is now two-fold symmetric, J_p vanishes unless p is a multiple of 2. By definition, $J_0 = 0$ for both horizontal and vertical because the chromaticities are zero. Some of the lower-order J_p's have been computed and are listed in Table I. The 2nd and 6th columns show the contributions of the quadrupoles, while the 3rd and 7th columns the contributions of the sextupoles. The total contributions including those from the dipoles are listed in the 4th and 8th columns. In the 5th and 9th columns*, we list the contributions of J_p's to their respective beat factor per unit momentum offset as is indicated in each term of the summation of Eq. (5.5) but not including the cosine term.

We notice that the J_0's are not exactly zero. This is because Eq. (5.5) is only first order; for example, the betatron function used inside the integral is only the unperturbed one. Nevertheless, this gives us a measurement of the error involved. The contributions of the sextupoles are exactly -4π times the chromaticities.

We see that the sextupoles do produce beat waves in the harmonic space. This is because they have not been placed at the proper phase advances for confinement or cancellation. The tunes of the lattice are $\nu_x = 21.0954$ and $\nu_y = 15.4433$, so that the important Fourier components are $p = 42$ for the horizontal and $p = 31$ for the vertical. Because of the two-fold symmetry of the lattice $p = 31$ does not occur. As for $p = 42$, the horizontal beat factor is not large because $2\nu_x$ is still far from 42. However, we do see the beat waves exhibit large magnitudes at $p = 28$ and $p = 56$. This comes about because each of the two straight sections has a vertical tune advance of ~ 0.60 which is not too far from the vertical phase advance of 0.53

*in Table I of Ref. 10, the numbers in the 5th and 9th columns are incorrect, They should be reduced by a factor of 4.

Table I: The horizontal and vertical J_p's of the INS lattice with dispersion suppressors, showing their contributions from the quadrupoles and sextupoles.

	Horizontal J_p				Vertical J_p			
p	quads	sext.	total	$\Delta\beta/\beta$	quads	sext.	total	$\Delta\beta/\beta$
0	−312.94	314.25	0.32	0.00	−261.12	265.00	2.78	−0.03
2	−2.09	8.29	6.24	−0.05	−6.14	10.66	4.41	−0.05
4	2.67	−75.48	−72.64	0.55	3.27	−66.49	−62.92	0.66
6	−1.53	−1.85	−3.35	0.03	−4.80	−1.09	−5.92	0.06
8	1.84	−57.84	−55.87	0.44	2.27	−48.40	−45.95	0.51
10	−0.48	−13.89	−14.35	0.11	−2.90	−12.32	−15.17	0.17
12	0.60	−38.61	−37.93	0.31	1.69	−34.09	−32.34	0.39
14	1.02	−17.37	−16.35	0.14	−1.44	−11.96	−13.33	0.17
16	−0.89	−27.41	−28.27	0.25	2.26	−29.05	−26.77	0.38
18	3.16	−3.08	0.06	0.00	−0.97	−1.64	−2.58	0.04
20	−2.33	−25.93	−28.25	0.27	3.70	−23.93	−20.22	0.36
22	7.00	34.65	41.66	−0.43	−0.98	5.68	4.69	−0.10
24	−2.48	−21.46	−23.94	0.27	3.81	2.21	6.03	−0.16
26	20.41	136.40	157.02	−1.91	0.20	−2.01	−1.82	0.06
28	37.47	237.37	275.37	−3.71	−16.50	178.65	162.33	−9.39
30	−32.55	−177.80	−210.80	3.22	−5.44	37.26	31.91	−5.81
32	−19.48	−99.22	−118.91	2.11	21.13	−78.39	−57.46	−8.07
34	−7.96	−21.06	−29.08	0.63	2.60	−3.02	−0.39	−0.02
36	−17.37	−57.92	−75.46	2.09	12.10	−19.49	−7.48	−0.21
38	−4.86	0.74	−4.09	0.16	6.41	−7.68	−1.31	−0.03
40	−16.10	−24.01	−40.22	3.00	6.61	−2.91	3.72	0.06
42	−5.94	9.72	3.85	−3.22	8.40	−6.06	2.25	0.03
44	−13.25	2.38	−10.91	−0.94	1.54	1.70	3.31	0.03
46	−10.72	30.29	19.66	0.79	8.11	−4.79	3.25	0.03
48	−8.45	14.10	5.65	0.14	−4.70	−2.50	−7.17	−0.05
50	−21.04	79.26	58.30	1.09	6.25	−3.09	3.16	0.02
52	−2.66	13.46	10.80	0.16	−15.97	−28.71	−44.72	−0.25
54	−50.08	206.72	156.67	1.85	3.69	4.46	8.20	0.04
56	−7.97	49.03	41.06	0.41	−53.71	−156.79	−210.63	−0.95
58	105.08	−395.70	−290.43	−2.46	−29.08	−82.47	−111.54	−0.46
60	21.14	−39.80	−18.63	−0.14	46.91	204.55	251.55	0.93
62	5.01	1.08	6.09	0.04	1.98	48.54	50.54	0.17

for each FMC module. On the other hand, their horizontal tune advances are 1.00 and 0.70, respectively, for the straights with dispersion and the one without. They average out to roughly the horizontal tune advance of a FMC module. Thus, the contributions of the sextupoles add up. As a result, there appears to be roughly a 7-fold symmetry in a superperiod. To reduce this contribution, the vertical phase advance of the straight section must be increased.

VI DISCUSSIONS

(1) One disadvantage of the dispersion-free lattice is the high bending field of the dipoles. There are ways to overcome this.

The easiest way is to lower the top operation energy of the machine. For example, acceleration up to 49 GeV will lower the peak bending field of 1.837 T to 1.800 T.

We notice that the peak field gradients of the quadrupoles are of the order of $0.1(B\rho\ \mathrm{Tm})\ \mathrm{Tm}^{-1} = 16.6\ \mathrm{Tm}^{-1}$. We can push the field gradient to a higher value and thus reducing the length of the quadrupoles. The length of each dipole can be lengthened accordingly. If we can increase the length of a dipole from 6.2 m to 6.3 m, for example, the maximum bending field will decrease to 1.808 T.

The main ring has a circumferential length of 17 rf wavelengths and the booster 4 rf wavelengths. If we increase the circumference of the main ring to 18 rf wavelengths, this amounts to an increase of 5.9%. With proper optimization, we can even pull out 4 more dipoles to make way for two more dispersion suppressors, so that all the long straight sections will be dispersion-free.

(2) One may not like the idea of chopping up a normal bending dipole into 2 halves in the dispersion suppressor. Unlike the FODO lattice, the ratio of the two halves is a little bit more flexible here, because we have more quadrupoles to play with. For example, it may be possible to divide that dipole up into the ratio of 2:1. Thus, if we are using 3 dipoles for each half FODO cell, there will not be any dipole chopping at all, although dipole lengths of 2 m are not economical.

(3) There may have been too many different types of quadrupoles used in this design, for example, some special ones in the dispersion suppressors and some special ones in the dispersion-free straights. Here, we have been using quadrupoles all with the same field gradient, except for the QDX at the entrance of the standard FMC

module and QFX at the center of the module. Our design has been a very rough one, and we do believe that with careful optimization, the number of special quadrupoles can be reduced.

(4) For this design, $2\nu_y + \nu_x = 51.982$ is too close to the third integer resonance. We have exactly the same situation for the original INS design without dispersion suppressors. However, we believe that this resonance can be avoided by a more careful design.

(5) The properties of the smears and beat factors are very similar to those of the original INS lattice. Therefore Sect. IV and V should be compared with the analysis made in Ref. 10.

APPENDIX

SYNCH input file

```
 MI_D  RUN
C
C                   INS MAIN RING with Dispersion-free Straights
C                             December, 1996
       SIZE   7



.----------------------------+---------------------------------------------
.          FACT is fraction of a whole dipole to be placed
.          at end of dispersion suppressor
 FACT  =            0.83

.          Quadrupoles for FCM
.
 QDXL  =            0.7500
 QFXL  =            1.0000
 QFL   =            0.7500
 QDL   =            0.7500
 GDX1  PARA         6.99753368-2
 GFX1  PARA         1.11841794-1
 GF1   PARA         7.76223575-2
 GD1   PARA         7.65636939-2
 GDX   =            GDX1      /         QDXL
 GFX   =            GFX1      /         QFXL
 GF    =            GF1       /         QFL
 GD    =            GD1       /         QDL
       PRNT   1    5 GDX  GFX  GF   GD
 QDX   MAG          QDXL      -GDX      1.
 QFX   MAG          QFXL      GFX       1.
 QF    MAG          QFL       GF        1.
 QD    MAG          QDL       -GD       1.


.          Dipole

.      The normal dipoles are called BB, the one at the end of
.      suppressor B4 and the left over part is B4E
```

```
NB     =           92.        /          2.
ANG    =           PI         /          NB
       PRNT   1   5 ANG

BL     =           6.20
BB     MAG         BL         0.         BL         ANG        $
.
FACT1 =            1.00       -          FACT
BL4    =           BL         *          FACT
BL4L   =           BL         *          FACT1
ANG4   =           ANG        *          FACT
ANG4L =            ANG        *          FACT1
B4     MAG         BL4        0.         BL4        ANG4       $
B4E    MAG         BL4L       0.         BL4L       ANG4L      $


.          Sextupoles
SDS    PARA        -8.9965455-2
SFS    PARA        5.8884901 -2
SXS    PARA        -0.105
SD     SXTP        0.0        SDS        1.
SF     SXTP        0.0        SFS        1.
SX     SXTP        0.0        SXS        1.

.          Markers

REF    DRF         0.0
RE1    DRF         0.0
RE2    DRF         0.0
RE3    DRF         0.0
RE4    DRF         0.0
RE5    DRF         0.0
ARST   DRF         0.0

.          Drifts

LBQ    DRF         0.55
LBQ2   DRF         0.75
LS     DRF         5.71875
LSQD   DRF         0.2
LSQF   DRF         0.2
LS2S   DRF         2.85
LDS1   DRF         0.1
```

```
LDS2  DRF         0.2
LGAP  DRF         0.1
GAP   DRF         1.
LB    DRF         0.275

.         Sextupoles Insertions

DTH   BML         LDS1 SD   LDS2 SD   LDS2 SD   LDS2 SD   LDS2 SD   LDS1
FTH   BML         LDS1 SF   LDS2 SF   LDS2 SF   LDS2 SF   LDS2 SF   LDS1
XTH   BML         LB   SX   LB

.         FMC Module and Arc

MOD1  BML         XTH  BB   LBQ2 QF   QF   LBQ  BB   LBQ2 QD   QD
                  LSQD DTH  LS2S FTH  LSQF QFX  REF

MOD2  BML         QFX  LSQF FTH  LS2S DTH  LSQD QD   QD   LBQ  BB
                  LBQ2 QF   QF   LBQ  BB   LBQ2

FMC   BML         QDX  MOD1 MOD2 QDX

.     CYC         FMC  AMPL SF   SD   .19204    .15919
      CYC         FMC  AMPL SF   SD   0.0       0.0


.         From FMC, compute the matching betax, betay, and disp


.FMC  MMM         FMC
BEX   BETA   2    .FMC
BEY   BETA  12    .FMC
DISP  BETA   5    .FMC
ALX   =           0.
ALY   =           0.
      PRNT   1   5 BEX  BEY  DISP
BETO  IBET        0.0       BEX       ALX       0.0       DISP      0.0
                  0.0       BEY       ALY       0.0       0.0       0.0

.          Insertion Straight
.          Quadrupoles for Straights

SBRO  SUB
LS1   DRF         6.1962572
LS2   DRF         5.9013912
```

```
 LS3   DRF          6.1054984
 LS4   DRF          5.6202491
 FS1L  =            .86167133
 DS1L  =            .76736325
 FS2L  =            .98869637
 DS2L  =            .81734213
 QFS1  MAG          FS1L      GF        1.
 QDS1  MAG          DS1L      -GD       1.
 QFS2  MAG          FS2L      GF        1.
 QDS2  MAG          DS2L      -GD       1.

 INS1  BML          QDX
                    LS1  QFS1 QFS1 LS2  QDS1 RE5  QDS1
                    LS3  QFS2 QFS2 LS4  QDS2 REF
 TB0   TRKB         INS1 BET0
       END

       SOLV   5   8 SBR0 TB0      OREF  99999  -10              0
                    AX        REF                          0.0       .000001
                    AY        REF                          0.0       .000001
                    DX        REF                          0.0       .000001
                    BY        RE5                          32.3      .03
                    S         REF                          30.6262   .00000001
                    LS1                           1 5.00   6.20      .001
                    LS2                           1 5.00   6.20      .001
                    LS3                           1 5.00   6.20      .001
                    LS4                           1 5.00   6.20      .001
                    FS1L                          1 .70    1.10      .001
                    DS1L                          1 .70    1.10      .001
                    FS2L                          1 .70    1.10      .001
                    DS2L                          1 .70    1.10      .001

 INS2  BML   -1     INS1
.INS2  BML          QDS2

 INSF  BML          INS1 INS2 FMC

       CYC          INSF AMPL SF   SD   0.0       0.0

.      Dispersion Suppressor

 SBR1  SUB
 LBB   DRF          4.9529547
 LSS   DRF          2.9847822
```

```
FFXL  =           1.0581615
DDL   =           .75640644
FFL   =           .75182717

QFFX  MAG         FFXL      GF        1.
QDD   MAG         DDL       -GD       1.
QFF   MAG         FFL       GF        1.
MOD3  BML         QDX  XTH  BB   LBQ2 QFF  QFF  LBQ  B4E  LBB  LBQ2
                  QDD  QDD  LSQD DTH  LSS  FTH  LSQF QFFX REF
TB1   TRKB        MOD3 BETO

      END

      SOLV   3   5 SBR1 TB1      OREF  99999  -10             0
                  DX        REF                          0.0       .000001
                  AX        REF                          0.0       .000001
                  AY        REF                          0.0       .000001
                  LBB                          1 1.0     6.5       .0001
                  LSS                          1 1.0     3.0       .0001
                  FFXL                         1 0.06    1.2       .0001
                  DDL                          1 0.07    1.2       .0001
                  FFL                          1 0.07    1.2       .0001

SBR2  SUB
F1Z   =           2.1247714
F2Z   =           .45839046
F3Z   =           1.2895852
F4Z   =           .35937249
LQD1  =           .78683700
LQF1  =           .79189430
LQDM  =           .76677618
F1    DRF         F1Z
F2    DRF         F2Z
F3    DRF         F3Z
F4    DRF         F4Z
QD1   MAG         LQD1      -GD       1.
QF1   MAG         LQF1      GF        1.
QDM   MAG         LQDM      -GD        1.
MOD4  BML         QFFX LSQF FTH  F1   DTH  LSQD QD1  QD1  F2   BB
                  LBQ2 QF1  QF1  F3   B4   F4   QDM  RE1
MISS  BML         MOD3 MOD4
TB2   TRKB        MISS BETO

      END
```

```
      SOLV   5    7 SBR2 TB2      0RE1  99999  -10              0
                    X         RE1                            0.0       .00000001
                    DX        RE1                            0.0       .00000001
                    AX        RE1                            0.0       .00000001
                    AY        RE1                            0.0       .00000001
                    BY        RE1                            32.3155669.0000001
                    F1Z                         1 1.8        3.5       .001
                    F2Z                         1 0.10       1.5       .001
                    F3Z                         1 0.10       1.5       .001
                    F4Z                         1 0.2        1.6       .001
                    LQD1                        1 0.2        1.0       .001
                    LQF1                        1 0.7        1.3       .001
                    LQDM                        1 0.7        1.1       .001

REV   BML   -1      MISS
SUPP  BML           MISS REV
      CYC           SUPP AMPL SF   SD   0.0       0.0

.     Making Zero-Dispersion Straight

.     Compute Twiss functions at matching point

SSIM  BML           REV  MISS
SSI   MMM           SSIM
BEX   BETA   2      SSI
BEY   BETA  12      SSI
DISP  BETA   5      SSI
      PRNT   1    5 BEX  BEY  DISP
ALX   =             0.
ALY   =             0.
BET1  IBET          0.0       BEX       ALX       0.0       -DISP     0.0
                    0.0       BEY       ALY       0.0       0.0       0.0

SBR3  SUB
F5    DRF           7.2821746
F6    DRF           6.4229531
F7    DRF           5.9297456
F8    DRF           6.0165902
LQD3  =             .65887323
LQF3  =             .68612193
LQD4  =             .69295034
LQF4  =             .68687394
LQD5  =             .70467076
```

```
QD3   MAG          LQD3      -GD       1.
QF3   MAG          LQF3      GF        1.
QD4   MAG          LQD4      -GD        1.
QF4   MAG          LQF4      GF        1.
QD5   MAG          LQD5      -GD        1.
STDF  BML          QD3  F5   QF3  QF3  F6   QD4  RE3  QD4  F7
                   QF4  RE4  QF4  F8   QD5  RE2
TB2   TRKB         STDF BET1

      END

      SOLV   5   9 SBR3 TB2     ORE2  99999  -10             0
                   AX        RE2                           0.0       .00000001
                   AY        RE2                           0.0       .00000001
                   S         RE2                           31.14690  .00000001
                   BX        RE4                           25.3966999.0000001
                   BY        RE3                           25.3552107.0000001
                   F5                          1 5.0       10.0      .1
                   F6                          1 5.0       10.0      .1
                   F7                          1 5.0       10.0      .1
                   F8                          1 5.0       10.0      .1
                   LQD3                        1 0.5       1.1       .01
                   LQF3                        1 0.5       1.1       .01
                   LQD4                        1 0.5       1.1       .01
                   LQF4                        1 0.5       1.1       .01
                   LQD5                        1 0.5       1.1       .01


STDR  BML   -1     STDF
DFST  BML          STDF STDR
      CYC          DFST


ARCR  BML          5(   FMC  )    MISS
SUPR  BML          INS2 ARCR STDF
SUPL  BML   -1     SUPR
SUP   BML          SUPR SUPL
RING  BML          SUP  SUP
      CYC          SUP  AMPL SF   SD   0.0       0.0
.     CYC          RING AMPL SF   SD   0.0       0.0

      STOP
```

References

[1] This analysis is based on the most recent lattice design released by the INS.

[2] S.Y. Lee, K.Y. Ng, and D. Trbojevic, Phys. Rev. **E48**, 3040 (1993).

[3] N. Merminga and K. Ng, *Analytic Expressions for the Smear due to Non-linear Multipoles*, Fermilab Report FN-505, 1989.

[4] D. Edwards, SSC Central Design Group Report No. SSC-22 (1985); T.L. Collins, SSC Central Design Group Report No. SSC-26 (1985).

[5] T. Collins, Fermilab Internal Report 84/114.

[6] K.Y. Ng, *Derivation of Collins' Formulas for Beam-shape Distortion due to Sextupoles using Hamiltonian Method*, Fermilab Report TM-1281 (1984).

[7] K.Y. Ng, *Distortion Functions*, KEK Report 87-11 (1987).

[8] N. Merminga and K. Ng, *Hamiltonian Approach to Distortion Functions*, Fermilab Internal Report FN-493, 1988.

[9] E.D. Courant and H.S. Snyder, Ann. Physics **3**, 1 (1958).

[10] K.Y. Ng, *Effects of Chromaticity Sextupoles on the INS Lattice*, Fermilab Internal Report FN-651, 1996. There are errors in Table I. See footnote on page 14.